

EXTRACTING GULLY FEATURES AND ITS DYNAMICS FROM HIGH SPATIAL RESOLUTION IMAGERY USING OBJECT BASED IMAGE ANALYSIS

R.B.V. Shruthi*, N. Kerle, V. Jetten

Department of Earth Systems Analysis, Faculty of Geo-Information Science and Earth Observation (ITC), University of Twente, Netherlands
shruthi@itc.nl, kerle@itc.nl, jetten@itc.nl

KEY WORDS: Soil erosion, Gully erosion, Object-based image analysis, OOA, Land degradation, High spatial resolution imagery

ABSTRACT:

Gully erosion is responsible for a substantial amount of soil loss and is generally considered an indicator of desertification. Hence, mapping these features provides essential information needed on sediment production, identification of vulnerable areas for gully formation, land degradation and environmental effects. This paper investigates the use of object-oriented image analysis to extract gully features from imagery, using a combination of topographic, spectral, shape/geometric and contextual information obtained from Ikonos-2 and GeoEye-1 data. A rule-set was developed and tested for a semi-arid to sub-humid region in Morocco. The accuracy of the feature extraction based on percentage of gully system boundary (GSB) was assessed for three sub-watersheds (SW1, SW2, and SW3). Changes in the GSB, in three different sub-watersheds, ranged from moderate (11% in SW2 and 21% in SW1) to a very high increase (91% in SW3). The percentage of GSB indicated negligible overestimations between the reference area and OOA area in SW1 (4%) and negligible underestimations in SW3 (-3%). However, the percentage of GSB in SW2 (24%) was overestimated due to the difference in visual abilities of a human operator digitizing highly complex gully system with fuzzy boundaries. In particular finer edges within the complex gully systems were better identified semi-automatically than was possible by manual digitization, suggesting higher detection accuracy. OOA-based gully mapping is quicker and more objective than traditional methods, and is thus better suited to provide essential information for land managers to support their decision making processes, and for the erosion research community.

1. INTRODUCTION

Gully erosion represents an important sediment source in a range of environments (Poesen et al., 2003) and is considered as one of the indicators of desertification (UNEP, 1994). Hence, mapping existing gullies and their activity over a period of time is crucial studying the effects of gully erosion, such as sediment production, land degradation, and its environmental and socio-economical effects. Field-based methods were used in the past until aerial photos and later satellite imagery became more readily available. Remote sensing-based mapping is the only practical approach for mapping gully features over large areas, given the variability in gully size, shape and occurrence (Knight et al., 2007), as well as the dynamic nature of gully-affected landscapes. It has been recognized that accurate identification of gullies is not possible without additional data or expert knowledge (Bocco and Valenzuela, 1993). In addition auxiliary information, such as geometric properties (shape, dimension, orientation and texture) and the spatial relationship with surrounding features, allows an approach fundamentally similar to the cognitive approach used in visual image assessment, but in a controlled and reproducible quantitative manner. This makes it possible to treat erosion features as spatial objects that can be characterized based not only on their geometric properties, but also on their spatial relationship with surrounding features. The potential of object-oriented image analysis (OOA) to map gully erosion features from high spatial resolution optical imagery (HRI) has rarely been explored. One of the objective of this study is to examine the potential of OOA to map complex gully erosion features using HRI. Identifying the dynamics in gully/gully systems with is another objective.

The method is tested for an area approximately 5 km² in the Sehoul commune region of Morocco.

2. DATA AND METHOD

2.1 Data used

The data used in the study are PAN and multispectral blue, green, red and near infrared (MSS) bands from Ikonos-2 and GeoEye-1 acquired on 31-07-2001 and 20-07-2009 respectively. In addition a digital surface model (DSM) generated using stereoscopic GeoEye-1 data (PAN-0.41 m resolution) acquired on 20-07-2009 is used in the study. An overview of the data used and the method followed is illustrated in figure 1.

2.2 Topographic derivatives

The first step was to generate the necessary data from the stereo-pair and spectral information. The photogrammetric software SAT-PP, developed by ETH Zurich (Zhang and Gruen, 2006), was used to generate a 1 m DSM from the GeoEye-1 stereo-pair, together with the rational polynomial coefficients (RPCs). Nine ground control points obtained from a differential GPS survey were used to improve the orientation result of the RPC model. A vertical root mean square error of 0.37 m was achieved. Further, a digital terrain model (DTM), representing only the earth surface excluding the above ground features, essential for quantifying topographic parameters was derived from the DSM. Local artifacts in the DSM, e.g. those resulting from scattered vegetation patches and buildings, were

removed to avoid large errors in DTM derivatives (Martha et al., 2010a). Particular areas such as streams and river where the vertex or elevation values appeared to be erroneous were also corrected manually using 3D break-lines. Next, TauDEM (Tarboton, 1997) was used to calculate the slope in radians, and the D-infinity flow direction (FD) and contributing area. FD was calculated based on the steepest outward flow direction using triangular facets centered on each grid cell, and apportions flow between neighbouring grid cells based on flow direction angles. It encodes the angles in radians, counter-clockwise from East as a continuous quantity between zero and 2π . The D-infinity (D_∞) contributing area (in the absence of a weight grid) represents the specific catchment area (SCA). It is the upslope area per unit contour length, taken here as the number of cells times grid cell size (cell area divided by one dimensional cell size). This assumes that grid cell size is the effective contour length (which is in this study, 1 m), and does not distinguish any difference in contour length depending upon the flow direction. Sine and Cosine of FD were later calculated in ArcGIS. Flow accumulation based terrain parameters are typically used to describe flow of material over gridded surface, i.e. to quantify flow intensity, erosion potential (Hengl et al., 2003). Stream power index (SPI) and sediment transport capacity index ($STcI$) were generated in eCognition Developer (Baatz and Schäpe, 2000) using slope and SCA .

$$SPI = SCA \cdot \tan(Slope) \quad (1)$$

$$STcI = \left(\frac{SCA}{22.13} \right)^{0.6} \cdot \left(\frac{\sin(Slope)}{0.0896} \right)^{1.3} \quad (2)$$

SPI is an indicator of the potential energy available to entrain sediment, such that areas with high SPI have a greater potential for erosion. Stream power can be calculated as the product of discharge and slope (Allan and Castillo, 2007), thus for SPI the catchment area is an indicator for potential discharge from the areas above a gully. The $STcI$ accounts for the effect of topography on erosion and identifies the potential sources and transportation of sediments (Hengl et al., 2003; Moore et al., 1993). $STcI$ is an indicator for transport capacity of suspended sediment, which is generally a nonlinear function of stream power, hence the power function shown in equation 2 (Hessel and Jetten, 2007; Rustomji and Prosser, 2001).

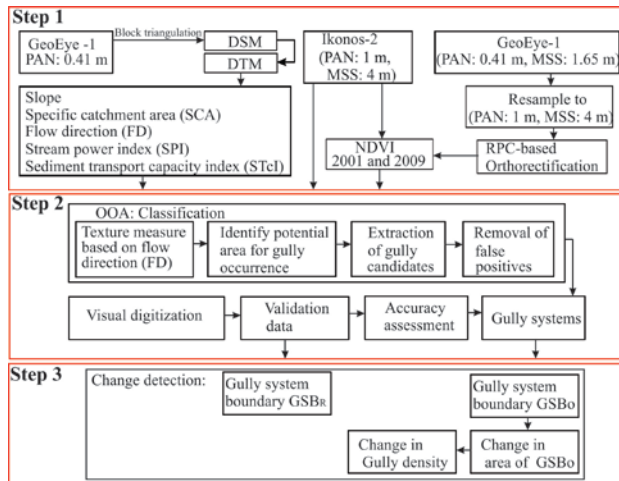


Figure 1: Overview of the method followed in this study

2.3 Gully feature extraction

The second step shown in figure 1 is the development of the rule-set for gully feature extraction within eCognition developer.

2.3.1 Texture measure (GLCM) based on flow direction:

First an optimal scale for multiresolution segmentation was estimated using the Estimation of Scale Parameter (ESP) method developed by Dragut et al., (2010). This was followed by averaging the angle of the flow direction (FD) within these segments. The average angle of the FD within these segments was later calculated using equations 3 and 4, and the angles converted from radian to degree.

$$\text{Average } FD \text{ angle within a segment} = \text{atan2}(y, x) \quad (3)$$

$$a \tan 2(y, x) = 2 \arctan \frac{y}{x + \sqrt{x^2 + y^2}} \quad (4)$$

Where, x : average cosine (FD), y : average sine (FD) with-in the segment.

Next, various texture measures (GLCM correlation and contrast) based on FD were calculated, and four direction classes classified: N-S; NE-SW; NW-SE and E-W.

$$GLCM_{COR\parallel} = \frac{\sum_{i,j=0}^{N-1} P_{i,j}(FD) \frac{(i - \mu_i)(j - \mu_j)}{\sqrt{(\sigma_i^2)(\sigma_j^2)}}}{\sqrt{(\sigma_i^2)(\sigma_j^2)}} \quad (5)$$

$$GLCM_{CON\perp} = \sum_{i,j=0}^{N-1} P_{i,j}(FD-90^\circ) (i - j)^2 \quad (6)$$

$$GLCM_{COR\perp} = \frac{\sum_{i,j=0}^{N-1} P_{i,j}(FD-90^\circ) \frac{(i - \mu_i)(j - \mu_j)}{\sqrt{(\sigma_i^2)(\sigma_j^2)}}}{\sqrt{(\sigma_i^2)(\sigma_j^2)}} \quad (7)$$

Where, i is the row number, j is the column number, N is the number of rows or columns, $P_{i,j}$ is the normalized value in the cell i,j , $\mu_{i,j}$ the mean of the texture, $\sigma_{i,j}$ the std. deviation of the texture within the segment.

2.3.2 Identifying potential areas of gully occurrence:

Areas that are on gentle to steep slopes ($> 5^\circ$), with relatively higher SCA ($\leq 55 \text{ m}^2/\text{m}$) and that are textured predominantly along the direction of flow ($GLCM_{COR\parallel} > 0.73$) were classified as potential areas of gully occurrence (PAGO) and were used for further analysis. Determining the thresholds of all the parameters was largely empirical based mainly on the spectral information and the local topographic variation. This was followed by additional multiresolution segmentation on the PAN and MSS images within PAGO with a scale factor of 41, as determined with the ESP tool. From the resulting objects, valley bottom gullies were extracted using a high SPI value (> 580), and by eliminating steeper slopes ($< 40^\circ$) and objects with a high length/width ratio (> 4), as they all are lengthier and extending almost throughout the sub-catchment. Subsequently the edges of the valley slope gullies were identified within the PAGO. To achieve this segments within the PAGO were further

segmented by chessboard segmentation with object size one. This segments the image into equal squares of a given size, in this case to re-establish the original image components (pixel level). The PAN data, the layer with the highest spatial resolution, were used to extract gully edges using a Canny edge detection filter at pixel level, keeping the default settings (Canny > 0). Later, the remaining PAGO were further segmented using multiresolution segmentation with a relatively small scale of 13 and using the PAN data (so that areas within the gully edges can form a segment of an individual gully). Lastly, a (prototype) contrast filter available with in eCognition was applied on the PAN data with a mean difference calculation mode at pixel level (contrast < 0) to extract valley slope gullies. It includes both simple and complex gully systems within the potential areas of gully occurrence and gully edge segments, with sufficient STel (≥ 1) (area indicating steeper slopes with smaller SCA or areas with larger SCA with moderate to gentle slope). All types of gullies as indicated in table 1 were extracted without distinguishing them as simple or complex gully systems. Finally the false positives were eliminated using a combination of different spectral, geometric and texture thresholds, based on process knowledge, such as *FD*. Figure 2 illustrates the steps adopted in gully feature extraction.

Similar procedure was followed and the developed rule-set with modified threshold was applied to Ikonos-2 data to extract the gully features. Due to their different spatial resolution, the optimal scale for multiresolution segmentation was different, and thus determined separately using ESP. However, the same topographic derivatives were used for both years for change analysis (generated from 2009 stereo image). The same procedure was followed for the second set of imagery. Texture along the direction of flow $GLCM_{CORII} > 0.84$ was used for identifying PAGO in the 2001 imagery as the image was captured on a different day, resulting in different spectral information than the earlier image. The rest of the parameters and thresholds remained the same for extracting potential valley bottom and valley slope gullies. Table 1 provides the criteria used for removal of false positives for both the imagery.

2.3.3 Quantifying changes in gully systems: Changes were quantified for a time difference of eight years, for three sub-watersheds one consisting of simple and continuous gully system (SW1), one consisting of a complex and discontinuous gully system on a concave slope (SW2), and a third system on a convex slope (SW3). Gully dynamics that quantification of change with regard to gully system boundary (i.e. the smallest convex polygon containing all the segments of a gully system, derived by a convex hull approach) and gully density were identified to be practical. Hence, polygons showing a GSB within each sub-watershed were generated by connecting the gully incision points using a convex hull approach. The feature outline masking application in the Cartography tool in ArcGIS, with a margin of 1m was used to generate the convex hull polygons, which were later aggregated to form one polygon. Convex hull polygons were generated for both the reference (GSB_R) (generated by visual interpretation) and OOA classified results (GSB_O) for the gully systems in 2001 and 2009. The difference in area estimates quantifies the change in the GSB. Gully density within the sub-watershed was calculated using measurement of total gully length (skeleton exported from OOA) per area of the sub-watershed. Gully density for the whole area was estimated using the line density tool in ArcGIS. The density was calculated as the ratio of total length of the

gully within the circular kernel (50 m search radius) by the total area of the circular kernel.

Criteria	False positives 2009	False positives 2001
Valley bottom gully		
Vegetation on steeper slope gradient	Slope > 20°, NDVI ≥ 0.45	Slope > 20°, NDVI ≥ 0.05
Low length by width ratio	Length/width > 2	Length/width > 2
Exposed soil and rocks	Brightness ≥ 320	Brightness ≥ 537
Valley slope gully		
Texture orthogonal to FD	$GLCM_{CORL} \leq 0.6$, $GLCM_{CONL} \leq 29000$	$GLCM_{CORL} \leq 0.4$, $GLCM_{CONL} \leq 1200$
Vegetation	NDVI ≥ 0.45	NDVI ≥ 0.04
Exposed soil and rocks	Brightness ≥ 320	Brightness ≥ 580
Low gully area	Area ≤ 3	Area ≤ 3

Table 1: Criteria for excluding false positives in two images

2.3.4 Accuracy of feature extraction: To verify the accuracy of the OOA based feature extraction, the same three sub-watersheds, SW1, SW2 and SW3 were chosen and their GSB. The difference between reference (GSB_R) (generated by visual interpretation) and classified data (GSB_O) was examined.

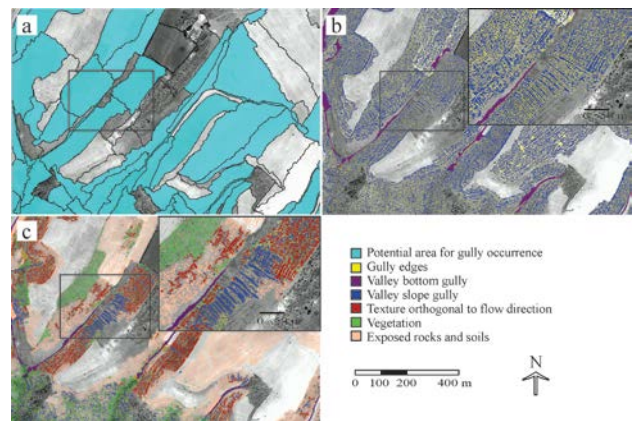


Figure 2: Steps adopted in the gully extraction on PAN for a subset area: (a) segments with potential areas of gully occurrence, (b) segments with valley bottom gully, gully edges and valley slope gullies, (c) false positives along with true gullies

3. RESULTS AND DISCUSSION

The rule-set estimated an area of 251,167 m² affected by gulying in the 2001 imagery, and about 294,760 m² in 2009, an increase in total gully area of 17% over eight years (figure 3). Table 2 provides the change in GSB for the three sub-watersheds from 2001 to 2009 for gullies extracted with the

OOA method. Figure 3 illustrates the gully system extracted for the whole area for the 2009 GeoEye-1 imagery.

Sub-Watershed	2001 GSB _O , m ²	2009 GSB _O , m ²	Change in GSB _O , % increase
SW1	9174	11077	21
SW2	60414	67159	11
SW3	8547	16348	91

Table 2: Change in GSB from 2001 to 2009, for gullies extracted from OOA

In case of SW1 (gully systems on moderate slopes) field investigations revealed the presence of pipes (form of sub-surface erosion resulting from flow through a discrete macropore) and gully head collapse, which increased the gully length and subsequently the GSB (figure 3a3 and a4). SW2, representing gully systems on steeper concave slope, despite having favorable topography and potential for collecting higher flow accumulation, displayed minimum change in the area of GSB (11%). This is mainly due to the fact that SW2 already displayed high degradation during 2001, and the upslope area available for gullies to retreat was limited. Hence, by 2009 only a minor increase in gully area occurred (figure 3b3 and b4). SW3 (representing gully systems on steeper convex slope) shows a higher % increase in area enclosed by GSB, about 91% (figure 3c3 and c4). The gully system in SW3 displayed backward erosion (gully headcut retreat).

In situations where the GSBs show very minimal change but show increasing erosion networks within the system boundary, gully density is a better characteristic than a simple change in area of GSB. SW3 showed higher increase in gully density than the other two sub-watersheds, about 109% increase over nine years. This is due to the presence of gully system on a steeper concave slope that favors higher flow accumulation zones. Similar conditions apply to the increase in density of the gully system in SW2, about 104%. SW1 showed a lower change in density value (81%), as it is located on moderate to gentle slope, and most of the upslope area is being used for cultivation. The area in the upslope of the gully system is prepared by ploughing, which helps in diverting the portion surface flow from headcut and reduces the effect of flow accumulation from the upslope area.

The overall gully density change map for the whole area is shown in figure 4a and b. Gully density during 2001 ranged from zero to 653 km/km², while by 2009 the density ranged from zero to 914 km/km². Gully systems on both steeper concave and convex slopes displayed an increase in density.

When comparing the manually digitized gully system outlines with the OOA results (table 3), the simple erosion structures extracted on gentle slopes (Figure 5a1 and a2) in SW1 show very good agreement, i.e. a negligible overestimation of only 4%. Also the results for more complex systems on a convex slope (Figure 5c1 and c2) as in SW3 are in good agreement, showing a negligible underestimation of -3%. SW2 (Figure 5b1 and b2) posed a greater problem, as indicated by substantial overestimation rates of 24%. However, the reason for the discrepancy is that visual mapping is unable to capture the weak signature of erosion traces, leading to comparatively small gully system areas. However, OOA was more effective in capturing

those finer erosion traces, leading to a more accurate identification of the gully system and a larger GSB. Hence, what appears to be error in the OOA processing actually illustrates the limitations of visual image interpretation (Shruthi et al., 2011)

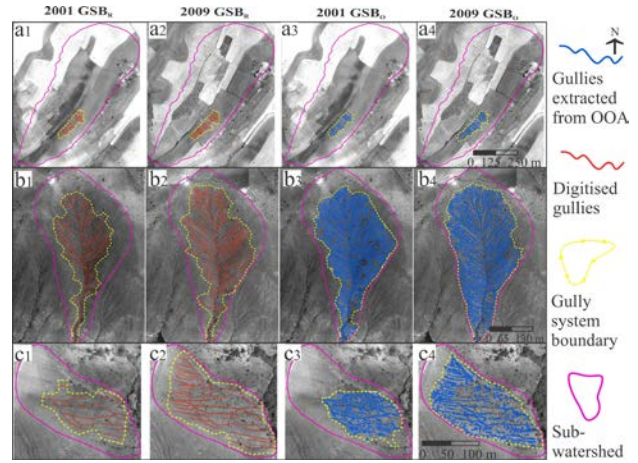


Figure 3: Changes in gully system boundaries (GSB) over a period of nine years in three different sub-watersheds. GSB for visually digitized gullies in 2001 (a1) and 2009 (a2), GSB for gullies extracted from OOA in 2001 (a3) and 2009 (a4) for SW1. Similarly (b1,2,3,4) and (c1,2,3,4) are for SW2 and SW3, respectively

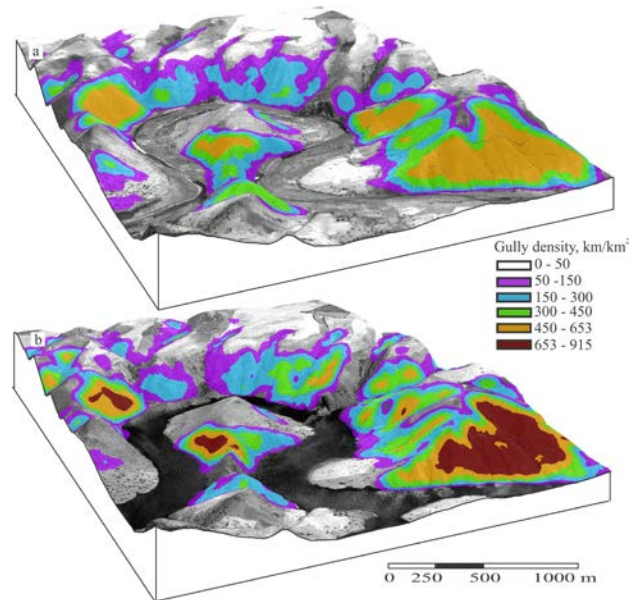


Figure 4: Map showing overall changes in gully density (km/km²) for the whole area in 2001 (a) and 2009 (b), overlaid on the DTM and panchromatic image

Sub-watershed	GSB _R , m ²	GSB _O , m ²	Difference in GSB, m ²	% over/under estimation
SW1	10658	11077	419	4
SW2	54110	67159	13049	24
SW3	16913	16348	-565	-3

Table 3: Difference in area of GSB between digitized reference gullies (GSB_R) and OOA extracted gullies (GSB_O)

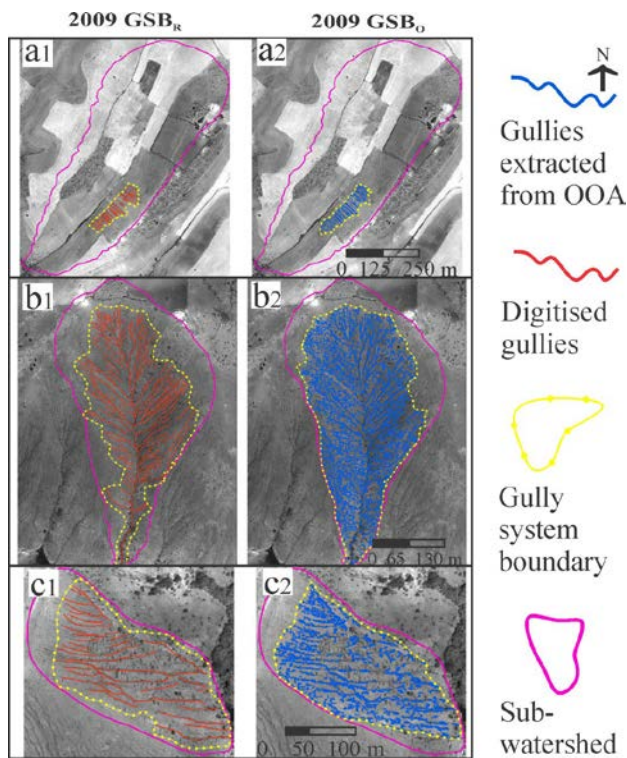


Figure 5: GSB of reference (digitization by visual image interpretation) and OOA data (output from the rule-set developed) for three different sub-watersheds displayed on PAN data of GeoEye-1 imagery. The gully system boundary (GSB) for gullies digitised for three different sub-watersheds from visual interpretation that forms the reference data is seen in a1, b1 and c1. GSB obtained from OOA based classification is seen in a2, b2 and c2.

4. CONCLUSIONS

Accurate and comprehensive information of gully erosion features is of critical importance for land managers and scientists. To achieve this we firstly need to know gully location and extent, and our study presents a method to provide this essential information. Our study suggests that OOA-based gully mapping is quicker and more objective than traditional methods, and is thus better suited to provide essential information for land managers to support their decision making processes, as well as for the erosion research community.

The thresholds used, however, remain largely empirical and require adaptation when the rule-set is used for a different region/imagery. Process knowledge is also used in removing the false positives; however, most of them are still removed based on image spectral information. This makes the rule-set sensitive to the thresholds used.

The rule-set established the topographical and image thresholds for a given area using not only spectral and textural information, but also considering process knowledge of soil erosion by overland flow. Averaging of the FD angle for a segment and assigned to one of the four directional classes to obtain texture information within the segments showed little

improvement in the texture calculation. This was mainly due to some of the features that appeared quasi-linear, mainly plough lines along the slope, cattle trails and exposed marl layers. The use of process related knowledge in the method improved the gully feature extraction. In this rule-set SPI was used to help distinguishing the long valley floor gullies, which coincides with the fact that these are flow erosion features occurring in locations where all catchment drainage occurs. The valley slope gullies, however, are a combination of flow erosion features and backward erosion (partly small mass movements), which are less linked to water than to sediment transport, hence the use of $STCI$.

The negligible over/under estimation can be due to a number of uncertainties related to the spatial resolution of the imagery used and the accuracy of the photogrammetric DTM, as well as the derivatives calculated from it. This especially concerns local slope values that are highly sensitive to artifacts.

The potential users of this approach are land managers interested in the location of gullies, the degree of land degradation, and gully dynamics over a period of time for the planning and implementation of soil conservation measures. The approach is also useful for the erosion research community, and can be further extended to provide more information such as gully dimensions and temporal changes of individual gullies and complex gully system networks. This required a clear definition of what constitutes change in a gully erosion context. The most practical and appropriate approach of change detection for a region with several complex networks of gully systems is based on the detection of GSB and gully system density within sub-watersheds. This study provides information on the location of gullies, gully dynamics over a period of time and the degree of land degradation (gully density) for developing and implementing soil conservation measures.

Reference

- Allan, J.D., Castillo, M.M., 2007. Fluvial geomorphology. Stream ecology: structure and function of running waters. Springer, Berlin.
- Baatz, M., Schäpe, A., 2000. Multiresolution segmentation-an optimization approach for high quality multi-scale image segmentation, *Angewandte Geographische Informationsverarbeitung XII*. Herbert Wichmann Verlag, Karlsruhe, Germany, pp. 12-23.
- Bocco, G., Valenzuela, C.R., 1993. Integrating satellite remote sensing and Geographic Information Systems technologies in gully erosion research. *Remote Sensing Reviews*, 7, 233-240.
- Dragut, L., Tiede, D., Levick, R.S., 2010. ESP: a tool to estimate scale parameter for multiresolution image segmentation of remotely sensed data. *International Journal of Geographical Information Science*, 24, 859-871.
- Hengl, T., Gruber, S., Shrestha, D.P., 2003. Digital Terrain Analysis in ILWIS. http://www.itc.nl/library/Papers_2003/misca/hengl_digital.pdf.
- Hessel, R., Jetten, V.G., 2007. Suitability of transport equations in modelling soil erosion for a small loess plateau catchment. *Engineering geology*, 91 56-71.
- Knight, J., Spencer, J., Brooks, A., Phinn, S., 2007. Large-area, high-resolution remote sensing based mapping of alluvial gully erosion in Australia's tropical rivers,

- Proceedings of the 5th Australian Stream Management Conference: Australian Rivers: Making a Difference, Charles Sturt University, Thurgoona, New South Wales, pp. 199-204.
- Martha, T.R., Kerle, N., Jetten, V.G., van Westen, C.J., Kumar, V., 2010a. Landslide volumetric analysis using Cartosat - 1 - derived DEMs. *IEEE Geoscience and Remote Sensing Letters*, 7, 582-586.
- Moore, I.D., Gessler, P.E., Nielsen, G.A., Peterson, G.A., 1993. Soil attribute prediction using terrain analysis. *Soil Science Society of America Journal*, 57, 443-452.
- Poesen, J., Nachtergaele, J., Verstraeten, G., Valentin, C., 2003. Gully erosion and environmental change: importance and research needs. *Catena*, 50, 91-133.
- Rustomji, P., Prosser, I., 2001. Spatial patterns of sediment delivery to valley floors: sensitivity to sediment transport capacity and hillslope hydrology relations. *Hydrological Processes*, 15, 1003-1018.
- Shruthi, R.B.V., Kerle, N., Jetten, V., 2011. Object-based gully feature extraction using high resolution imagery. *Geomorphology*, 134, 260-268.
- UNEP, 1994. United Nations Environmental Programme. United Nations Conventions to Combat Desertification in Those Countries Experiencing Serious Drought and/or Desertification, Particularly in Africa, Geneva, Switzerland.
- Zhang, L., Gruen, A., 2006. Multi-image matching for DSM generation from IKONOS imagery. *ISPRS Journal of Photogrammetry and Remote Sensing*, 60, 195-211.

Acknowledgement:

We wish to thank the DESIRE project for providing funds for conducting this study. We also thank Prof. Laouina Abdellah and his team, UNESCO-GN Chair, Univ. Mohammed V-Agdal, Rabat, for providing logistical support during the field work.